Isolation of Bidimensional Electron Gas in AlGaN/GaN Heterojunction using Ar Ion Implantation

Antonino Scandurra[a,b,c,*], Matteo Testa[a], Giorgia Franzò[b], Giuseppe Greco[d], Fabrizio Roccaforte[d], Maria Eloisa Castagna[e], Cristiano Calabretta[e], Andrea Severino[e], Ferdinando Iucolano[e], Elena Bruno[a,b,c] and Salvatore Mirabella[a,b]

[a] Department of Physics and Astronomy "Ettore Majorana", University of Catania, via Santa Sofia 64, 95123 Catania, Italy;

[b] Institute for Microelectronics and Microsystems of National Research Council of Italy (CNR-IMM, Catania University Unit), via Santa Sofia 64, 95123 Catania, Italy;

[c] Research Unit of the University of Catania, National Interuniversity Consortium of Materials Science and Technology (INSTM-UdR of Catania), via S. Sofia 64, 95125 Catania, Italy;

[d] Institute for Microelectronics and Microsystems of National Research Council of Italy (CNR-IMM), Ottava Strada, 5 (Zona Industriale) - 95121 Catania (CT) Catania, Italy;

[e] STMicroelectronics, Stradale Primosole 50, 95121 Catania, Italy;

*Corresponding author antonino.scandurra@dfa.unict.it

Abstract

Gallium nitride (GaN) has superior physical properties suitable for the realization of power switching and high-frequency transistors with better performances than of conventional Si-based devices. In the presence of a bidimensional electron gas (2DEG) close to the interface of AlGaN/GaN heterojunctions, High Electron Mobility Transistors (HEMT) can be fabricated. Ion implantation is an affordable industrial process for the electrical isolation of 2DEG in adjacent AlGaN/GaN HEMTs devices. In this work, we studied the electrical isolation of the 2DEG produced by Ar ion implantation. 2DEG of heterostructure consisting of 18 nm $Al_{0.2}Ga_{0.8}N$ were grown onto carbon doped n-type GaN. The 2DEG has been isolated by Ar ions implantation at 15, 22.5 and 60 keV and fluence of 7×10^{13} cm^{-2}, respectively. The implanted samples were annealed at 600, 750 and 900 °C, respectively, and the thermal stability of the crystal damage and isolation were analyzed by photoluminescence spectroscopy (PL) and capacitance-voltage profiling (CV) through mercury probe analysis. We found that Ar ion implantation at the explored ion energies and fluence produces a significant reduction of the PL peak intensity assigned to radiative recombination at the band edge of GaN, confirming the crystal lattice damage induced by the implant. The PL spectral features are matched by a significant reduction of the 2 DEG carrier density of about six orders of magnitude with respect to the undamaged sample. The reduction of carrier density and, then, the isolation of the 2DEG was found stable at temperature up to 900°C.

Keywords: gallium nitride, 2DEG isolation, ion implantation, photoluminescence, mercury probe.

Introduction

Gallium nitride (GaN) has superior electrical, mechanical and thermal properties than silicon, in terms of e.g. wide band-gap, high carrier concentration, high electron mobility, high saturation velocity with high critical electric field strength, thermal conductivity and Young's modulus [1-8]. These properties make suitable GaN for the realization of power high-frequency transistors with better switching performance and reduced power loss than conventional Si-based devices [9]. In particular, GaN allows the fabrication of AlGaN/GaN heterojunctions, where a fraction of Ga atoms is replaced in the crystal structure by Al atoms. Heterojunction results in a spontaneous, very high sheet carrier density named bidimensional electron gas (2DEG). The carrier density is produced by the different electronegativity of Al, Ga and N and the presence of piezoelectric polarization at the GaN/AlGaN interface due to the mismatch of the crystal lattice parameters [10,11]. The 2DEG can be exploited in the fabrication of high electron mobility transistors (AlGaN/GaN HEMTs). Mesa etching is a typical process used for the isolation of adjacent devices or to define active regions. It consists in the reactive ion etching of the thin AlGaN layer down to the underlying GaN using chlorine-based plasmas with the effect of cutting the 2DEG [12]. However, mesa isolation presents several drawbacks since it is not a planar process and may cause an increase of gate leakage current, decreasing the device breakdown voltage. This may occur through the contact of gate metallization and transistor channel at mesa edge [13].

Conversely, ion implantation is an affordable planar process for the electrical isolation of 2DEG for the inter-device isolation in adjacent AlGaN/GaN heterostructures. Different ions, ranging from non-reactive noble gases (Ar, Kr, Xe,) [14,15] to reactive species (H, Li, B, C, O, F, Al, Fe) are reported in the literature for the 2DEG isolation [16-21]. Table 1 summarizes the typical ions, energies and fluences, reported in literature, utilized for the isolation of 2DEG. In principle, all the ions reported in Table 1 are effective in producing the electrical isolation of the 2DEG. However, the main difference among the various ion species concerns the temperature stability of the isolation. The

required temperature stability of the isolation depends on the flow chart of specific device fabrication. Typically, the 2DEG isolation is considered acceptable in the range of temperature 300 to 600 °C. This is related to some high-temperature fabrication steps of AlGaN/GaN HEMTs, such as the realization of Ohmic contacts in metal-GaN or device passivation. At high temperature the lattice damage produced by ion implantation can be partially recovered, producing a decrease in the resistance of the implanted region and, hence, a degradation of its isolation capability.

Table 1. Type of ion, energy, fluence and isolation stability reported in literature for the isolation of 2DEG by ion implantation.

Ion	Energy (keV) [(1)]	Fluence (cm^{-2}) [(1)]	Thickness of AlGaN (nm)	Sheet resistance Ω/sq. or current leakage $nAmm^{-1}$ (@temperature)	Reference
Xe^+	5 15 30 45 100	$5\cdot10^{13}$; $1\cdot10^{13}$; $1\cdot10^{13}$; $1\cdot10^{13}$; $1\cdot10^{13}$	2(GaN)cap 18 AlGaN	$9.4\cdot10^{11}$ Ω/sq. isochronal RTA (500, 600, 700, 800°C)	16
Xe^+	5 15 30 45 100	$5\cdot10^{13}$; $1\cdot10^{13}$; $1\cdot10^{13}$; $1\cdot10^{13}$; $1\cdot10^{13}$	2(GaN)cap 18 AlGaN	$2\cdot10^{7}$-10^{10} Ω/sq. (300-420 K)	16
Kr^+	5 25 45	$7.4\cdot10^{12}$; $7.1\cdot10^{12}$; $1.1\cdot10^{13}$	20	2.4 (700°C) Ibuffer 2.4 (800°C)	15
Ar^+	5 25 45	$4.2\cdot10^{12}$; $6.3\cdot10^{12}$; $1.1\cdot10^{13}$	20	6 (700°C) Ibuffer 10 (800°C)	15
C^+	800 300 520 250	$1.5\cdot10^{13}$ $1\cdot10^{13}$ $5\cdot10^{13}$ $4\cdot10^{13}$	2(GaN)cap 26 AlGaN	$5.8\cdot10^{11}$ Ω/sq. (as impl.) $6.2\cdot10^{13}$ Ω/sq. (400°C) $1\cdot10^{13}$ Ω/sq. (600°C) $6.3\cdot10^{7}$ (800°C)	16
Al^+	800 300 520 250	$1.5\cdot10^{13}$ $1\cdot10^{13}$ $5\cdot10^{13}$ $4\cdot10^{13}$	2(GaN)cap 26 AlGaN	$1.8\cdot10^{11}$ as impl. $1.2\cdot10^{14}$ Ω/sq. (400°C) $3\cdot10^{12}$ Ω/sq. (600°C) $1.5\cdot10^{8}$ Ω/sq. (800°C)	16
N^+	30 160 400	$6\cdot10^{12}$ $1.8\cdot10^{13}$ $2.5\cdot10^{13}$	2.5 (GaN) cap 20 AlGaN	$8\cdot10^{11}$ Ω/sq (550 °C)	17
O^+	25 50 75	$5\cdot10^{14}$ $5\cdot10^{14}$ $5\cdot10^{14}$	30	$1\cdot10^{12}$ Ω/sq (450°C)	18
Fe^+	40 83 200	1-$9\cdot10^{12}$	1 (GaN) cap 25 AlGaN	$2\cdot10^{15}$ Ω/sq (400-1100°C)	19

Fe$^+$	40 83 200	$1\text{-}9\cdot10^{13}$	1 (GaN) cap 25 AlGaN	$1\cdot10^{14}$ Ω/sq (400-1100°C)	19
Fe$^+$	50	$3\cdot10^{13}$	25 nm AlGaN	$1\cdot10^{10}$ Ω/sq (1000-1200°C)	20
F$^+$	10	$1\cdot10^{14}$	25 nm AlGaN	I_{sat} /$I_{leakage}$ 10^8 (400 °C)	21
B$^+$	20	$1\cdot10^{14}$	25 nm AlGaN	I_{sat} /$I_{leakage}$ 10^8 (400 °C)	21

(1) The values in the same line refer to multiple energy and multiple fluence ion implantations;

The isolation mechanisms proposed in literature are based on the formation of intentional damaged lattice, especially at the AlGaN/GaN interface. The defects in the damaged lattice at the AlGaN/GaN interface trap the free electrons, locally inhibiting the 2DEG. This mechanism is present in all the kinds of ions reported in literature. In addition, for some ions, such as O, C and Fe, the isolation is attributed to further mechanism consisting in the formation of deep levels [16,19,20].

However, the results concerning the thermal stability of 2DEG electrical isolation by ion implantation as well as the mechanisms described in literature up to date are, often, not unambiguous. Most of the literature data are based on the employment of devices where the 2DEG is contacted using metal pads [14-21]. Temperature dependence of the specific electrical resistance of metal contact on n-type GaN, due to the chemical modification or inter-diffusion at the interface between the GaN and the metal pad, should be accounted apart the effects attributable to the ion implantation itself on the 2DEG [22]. Noteworthy, the quality of the 2DEG as well as its destruction can be monitored by measuring the intensity of the peak assigned to the radiative recombination of pairs at the band edge (BE) observed by the photoluminescence spectroscopy (PL). The intensity ratios between the yellow band (YL) or blue band (BL) and the BE respectively are suitable indicators to estimate the device performances [23].

In this work, we studied the 2DEG electrical isolation and its thermal stability up to 900 °C produced by argon ion implantation. Ar was preferred over the other species as it does not have secondary

effects on the semiconductor. Ar ions were implanted at different energies into an AlGaN/GaN heterostructure with 18 nm thick AlGaN barrier layer. We used a cost-saving procedure based on the wafer level measurements of photoluminescence peak assigned to radiative recombination of donor-acceptor pairs at the band edge. The electrical isolation and its thermal stability have been measured by capacitance-voltage profiling through mercury probe (CV). This approach avoids the use of thermal annealed metal contacts and the related interface effects, minimizing the effects at the semiconductor-metal pad interfaces in the electrical characterization of the 2DEG. The implanted samples were annealed at 600, 750 and 900 °C, respectively, and the isolation stability at different temperatures was analyzed by PL and CV.

Experimental

Layer of $Al_{0.2}Ga_{0.8}N$ 18 nm thin, with a GaN capping layer 1 nm thin, were grown onto carbon doped n-type GaN by metal-organic chemical vapor deposition (MOCVD). The $Al_{0.2}Ga_{0.8}N$/GaN heterostructure was grown onto six-inches Si 111 substrates. The wafers were grinded to a thickness of 400 μm and then sawed into 20 mm × 20 mm dice. Previous to ion implantation process, simulation was done by SRIM software [24]. The ion energies have been chosen in order to have the concentration peak of the vacancy defects located at a smaller depth, equal to, or greater than that of the $Al_{0.2}Ga_{0.8}N$/GaN interface, i.e. 19 nm. Figure 1 shows the cross section of the heterostructure with the region involved in the ion implantation highlighted. Ion implantations were done at room temperature, by an ion implanter equipped with Cockroft-Walton linear accelerator, operating in the voltage range between 10 and 400 kV, (High Voltage Engineering Europa BV).

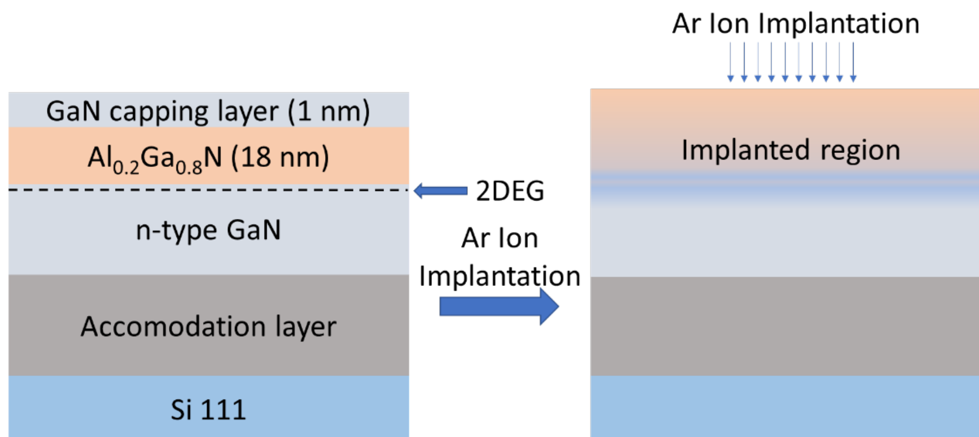

Figure 1. Cross section of the $Al_{0.2}Ga_{0.8}N$/GaN heterostructure with the region involved by the ion implantation highlighted. The thicknesses of the various layers are not to scale.

Thermal annealing was done in a Carbolite Gero tubular oven at 600, 750 and 900 °C, respectively, under N_2 flux at ambient pressure, for 15 minutes. The samples were cooled down at room temperature under N_2 flux and then withdrawn of the oven. Photoluminescence characterization was

done at room temperature by Nanometrics RPM 2000 Photoluminescence Mapper. Nd-YAG laser operating at a wavelength of 266 nm was used as excitation source.

Capacitance-voltage characterization was done by mercury probe CVmap 92 A/B by Four Dimensions Inc.

Results

Table 2 shows the conditions of energy and fluence of Ar ion implantation of the $Al_{0.2}Ga_{0.8}N$/GaN heterostructure, adopted in this study. The ion range and straggle values were obtained by SRIM simulation. Figure 2 shows the simulated defects concentration profiles obtained by ion implantation at the energies of 15, 22.5 and 60 keV and fluence of 7×10^{13} cm^{-2}, respectively.

Table 2. Energy and fluence conditions used in the Ar ion implantation. Ion range and straggle were obtained by SRIM simulation of Ar implanted in $Al_{0.2}Ga_{0.8}N$/GaN at different energies.

Energy (keV)	**Ion range (nm)**	**Straggle (nm)**	**Fluence (cm^{-2})**
15	19.3	9.5	7×10^{13}
22.5	26.7	13.3	7×10^{13}
60	64.0	28.4	7×10^{13}

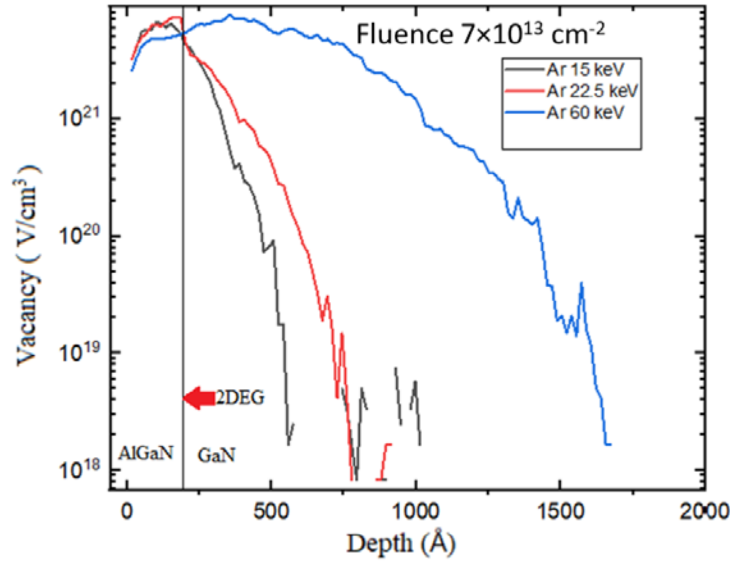

Figure 2. SRIM Simulated vacancy concentration profiles produced in $Al_{0.2}Ga_{0.8}N$/GaN heterostructure by Ar ion implantation at the energies of 15, 22.5 and 60 keV and fluence of 7×10^{13} cm^{-2}. The position of the 2DEG at the depth of 19 nm is indicated by the arrow.

We studied the effects of the solely thermal annealing at 600, 750 and 900 °C. The aim was to discern any effects strictly related to the thermal treatment from those related to the ion implantation. Figure 3a- d show the survey PL spectra in the range of 250-850 nm of wavelength of the reference and annealed at 600, 750 and 900 °C samples, respectively.

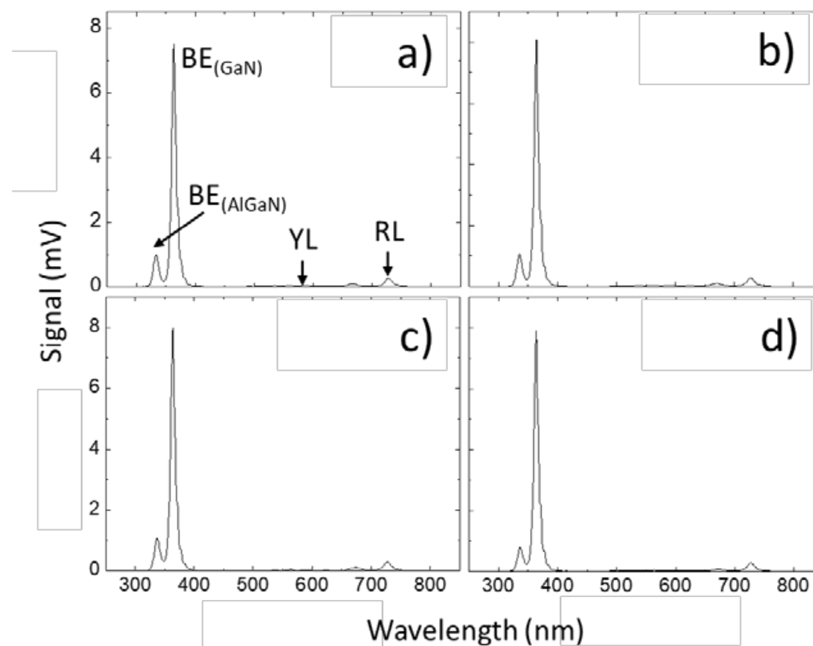

Figure 3. Photoluminescence spectra acquired at room temperature of $Al_{0.2}Ga_{0.8}N$/GaN: a) reference (as grown); b) annealed at 600 °C; c) annealed at 750 °C; d) annealed at 900 °C.

The spectra show an intense and narrow peak centered at about 363.3-363.8 nm, which is assigned to BE of GaN, a less intense peak centered at about 335 nm, assigned to BE of $Al_{0.2}Ga_{0.8}N$, a weak band comprises between 500 and 650 nm of wavelength assigned to YL. The YL band is attributed to donor to acceptor radiative recombination process at the defects consisting of carbon impurities in the nitrogen substitution position (C_N) [25]. Furthermore, a weak band between 650 and 750 nm of wavelength assigned to red luminescence (RL) is observed. The RL is attributed to clusters consisting of Ga vacancies (V_{Ga}) and N vacancies (V_N), e.g. $V_{Ga}(V_N)_2$ [26].

The enlarged regions of the PL spectra of reference and annealed samples in the ranges of 320-385 and 450-650 nm of wavelength are reported in Figure 4a-b, respectively. The alternating intensity of the YL of Figure 4b is the consequence of some photon diffraction mechanisms observed in our samples at those wavelengths.

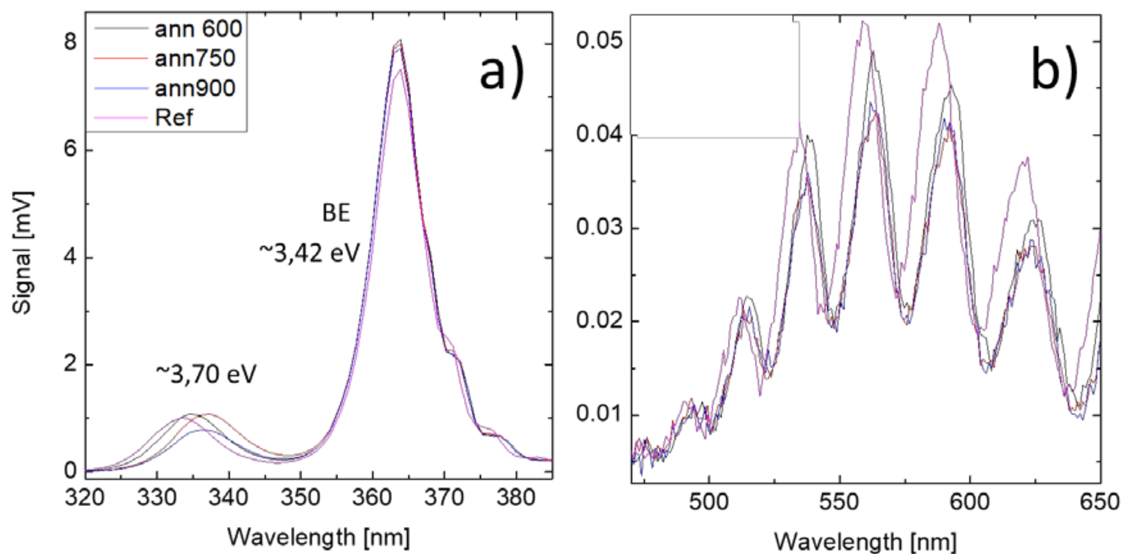

Figure 4. Photoluminescence spectra acquired at room temperature of the reference and the annealed samples: a) range of 320-385 nm of wavelength. The spectra show the peak at about 363.3-363-8 nm, assigned to band edge in GaN, and a weak peak at about 335 nm assigned to band edge of $Al_{0.2}Ga_{0.8}N$; b) range 450-640 nm of wavelength showing the yellow band (YL).

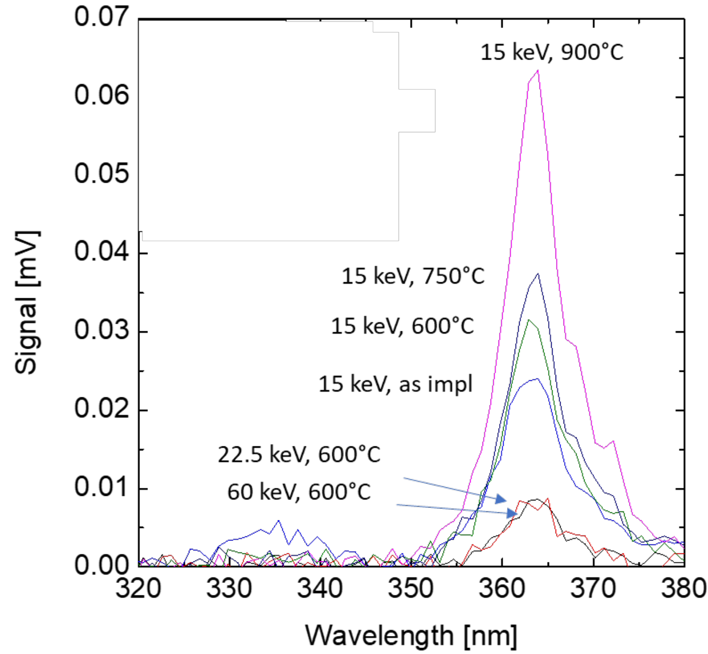

Figure 5. Photoluminescence spectra acquired at room temperature of the BE region of implanted and post-annealed $Al_{0.2}Ga_{0.8}N$/GaN samples. The relative intensities of the BE peaks are reduced by a factor 100 even in the 900 °C annealed sample, with respect to the reference sample (Figure 2a), indicating the destruction of the 2DEG and the stability of isolation at this temperature.

Figure 5 shows the PL spectra, comprising the BE of $Al_{0.2}Ga_{0.8}N$ and GaN, of Ar implanted and post- annealed samples. In all the spectra the BE of GaN is reduced in intensity by a factor 100 or more with respect to the spectra of reference and solely annealed samples (vide Figure 4a). Figure 6a-d shows the CV profiles corresponding to the reference, annealed at 600 and 900 °C, and implanted at 15 keV and post-annealed at 900 °C samples. In the implanted samples the capacitance is significant reduced to values that are below the instrumental measurement capability

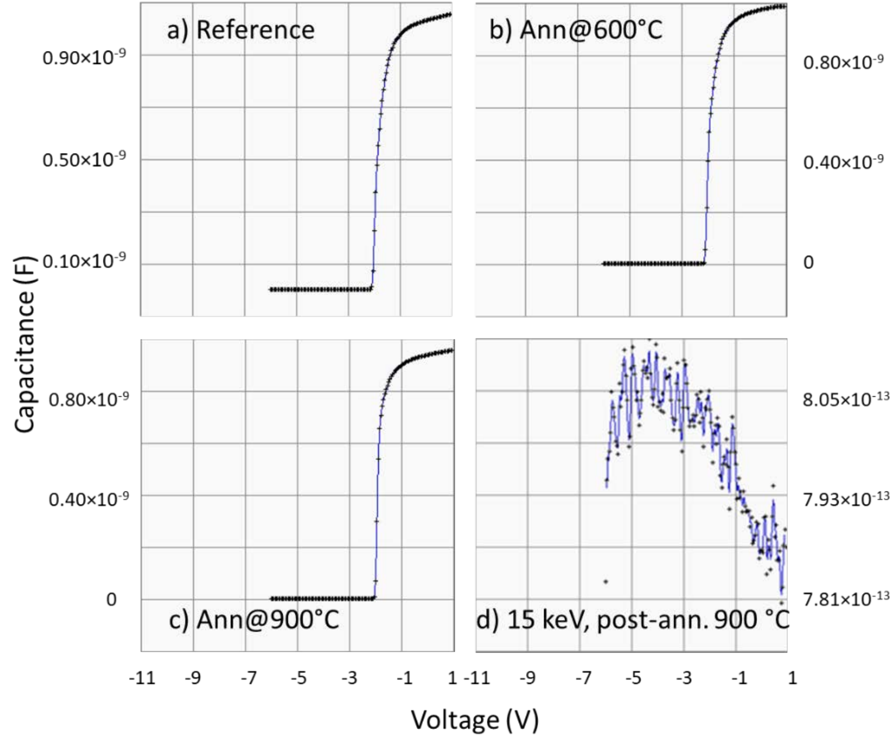

Fig. 6. Capacitance-voltage profiles of $Al_{0.2}Ga_{0.8}N$/GaN heterostructure obtained by mercury probe analyses of: a) reference; b) annealed at 600 °C; c) annealed at 900 °C; d) implanted at 15 keV and post-annealed at 900 °C. In the implanted samples the capacitance values are below the instrumental measurement capability.

Figure 7 reports the carrier concentration depth profiles of $Al_{0.2}Ga_{0.8}N$/GaN heterostructure of reference and annealed at 600, 750 and 900 °C, respectively, obtained by elaboration of the CV measurements basing on the Mott-Schottky Equation 1:

$$N_{CV} = \frac{C^3}{e\varepsilon_0\varepsilon}\frac{dV}{dC} \qquad \text{Eq. 1}$$

where N_{CV} is the carrier concentration, C is the capacitance, V the voltage, *e* the elemental charge, ε_0 the dielectric constant of vacuum and ε the relative dielectric constant.

The carrier concentration as function of depth can be calculated by the Equation 2:

$$z_{CV} = \frac{\varepsilon_0\varepsilon}{C} \qquad \text{Eq. 2}$$

In Figure 7, the carrier concentration corresponding to the 2DEG has been highlighted by the arrow. The carrier concentrations Nmax of the 2DEG and the corresponding depth (z) calculated by the Eq.

2 in the reference and as function of the annealing temperature, the energy of ion implantation and the post-annealing temperature are reported in Table 3.

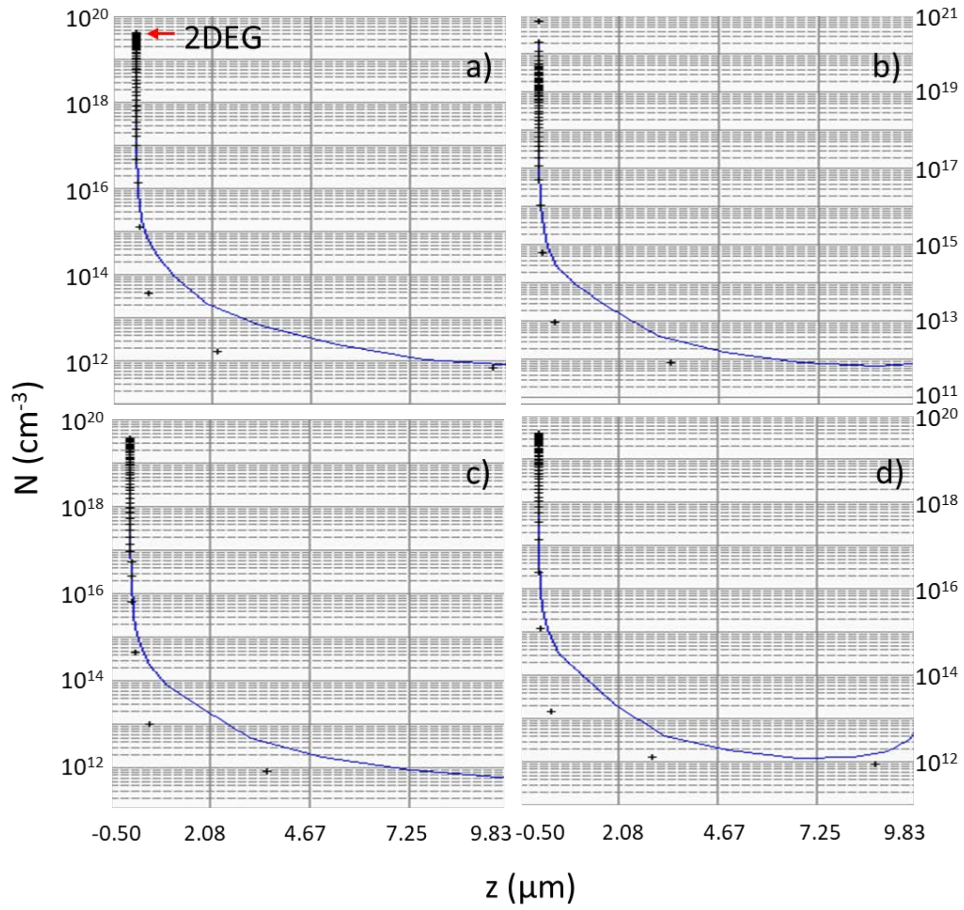

Fig. 7. Carrier concentration depth profiles of $Al_{0.2}Ga_{0.8}N$/GaN heterostructure obtained by Mott-Schottky elaboration of the CV measurements: a) reference; b) annealed at 600 °C; c) annealed at 750 °C; d) annealed at 900 °C. The red arrow indicates the carrier profile concentration attributable to the 2DEG.

Table 3. Carrier concentration (Nmax) and the depth (z) corresponding to the 2DEG in the various investigated samples, obtained by Mott-Schottky calculation based on the CV profiles.

Sample description	**Energy of Ar implantation (keV)**	**Fluence (cm^{-2})**	**Annealing temperature (°C)**	**Carrier concentration Nmax at 2DEG (cm^{-3})**	**z at Nmax (nm)**
Reference	-	-	-	3.98×10^{19}	23.5
Annealed only	-	-	600	6.7×10^{20}	24.7
Annealed only	-	-	750	3.69×10^{19}	26.5
Annealed only	-	-	900	3.89×10^{19}	25.7
Ar 15 keV	15	7×10^{13}	As implanted	$<1\times10^{13}$	-
Ar 15 keV	15	7×10^{13}	600	$\sim1\times10^{14}$	-
Ar 15 keV	15	7×10^{13}	750	$\sim1\times10^{14}$	-
Ar 15 keV	15	7×10^{13}	900	$\sim1\times10^{14}$	-
Ar 22.5 keV	22.5	7×10^{13}	600	$<1\times10^{14}$	-
Ar 60 keV	60	7×10^{13}	600	$<1\times10^{14}$	-

Discussion

The energies of 15, 22.5 and 60 keV of the Ar ion implantation were selected for this study with the aim to explore the effects of different level of damage that take place at depths close to the 2DEG. According to Usman and co-workers [27] Ar ion implantation of GaN produces a significant higher concentration of nitrogen defects than gallium defects, due to the smaller displacement energy of N compared to Ga [27]. In this study, the selected conditions of Ar ions implantation produce similar peak concentration of total vacancies of about 7×10^{21} cm^{-3}. However, the peak concentration of vacancy is located at different depths, depending on the energy of the implanted ion. Since Ar is a heavier ion mass than N, displacement occurs toward a shallower depth than the projected range of the implanted ion. Accordingly, the vacancy concentration peaks are located at shallower depth with respect to the projected ranges of Ar ions. The BE peaks assigned to GaN and AlGaN, respectively, do not show significant changes both in intensity and position under the solely thermal treatment up to 900 °C, indicating a good stability of our samples in the adopted conditions. Several authors have

shown that the photoluminescence peak assigned to BE is a diagnostic parameter of the quality of 2DEG [23, 26-28]. In particular, Zhong and co-workers [23] reported that epitaxial wafers characterized by low intensity of the YL to BE and blue luminescence (BL) to BE ratios values, combined with the carbon concentration, results in valuable primary indicators for estimating the device performance before design and fabrication. The reduction in PL intensity in ion implanted samples is attributed to the formation of non-radiative recombination centers as a consequence of damage to the crystal lattice [28]. Notable, the BE intensity increases slightly compared to the implanted sample as the temperature of the post-annealing process increases. This result can be attributed to partial recovery of crystalline damage. The presence of crystal defects results in a significant effect on the carrier density of the 2DEG, since they trap the carries and, then, increase the sheet resistance. Often, the effects of ion implantation on the electrical properties of the 2DEG have been studied by using HEMT transistor or test structures with metal contacts such as Ti/Al, Ti/Al(Ni)/Au or other equivalent [14-21,29]. However, at the temperature of 600 °C, the metal contacts likely show rectifying Schottky contact behavior and become ohmic by thermal process at temperatures above 600 °C. The interface microstructure modification, involving the metal and semiconductor elements at the temperature higher than 600°C, required to form an Ohmic rather than a Schottky contact, is responsible for the modification of the carrier transport mechanism [29]. The change in the carrier transport mechanism at the metal- n-type GaN contacts can introduces additional contribution in the measurements of the isolation of 2DEG in the temperature range of 600-900 °C. The additional contribution can affect a good data interpretation [30]. To overcome the latter contributions, we characterized the electrical isolation and the temperature stability of the 2DEG by CV profiling using the mercury probe technique. Thus, the $Al_{0.2}Ga_{0.8}N$/GaN implanted and post-annealed samples were not subjected to further thermal budget, required by annealing of metal contacts, rather than that to study the 2DEG thermal stability. The CV profiles of the samples subjected to solely annealing does not show significant variations of the carrier concentration of the 2DEG with respect to the reference up to 900 °C.

We can hypothesize that the annealing at lower temperature (600 °C) induce an improvement in the crystal quality due to the reduction of the concentration of point defects and dislocations, allowing the detection of a greater concentration of 2DEG with respect to the reference sample. Further increase in the annealing temperature has the opposite effect by inducing the partial modification of the AlGaN layer, visible in the PL in the AlGaN peak region, and the consequent reduction of the 2DEG concentration [31]. Conversely, the CV characteristics of the implanted and post-annealed samples show a significant reduction in the capacitance value down to the instrumental measurement capability. According, this result can be explained with the degradation of the 2DEG. In particular, the ion implanted samples show a descrese of the carrier concentration of the 2DEG of about six orders of magnitute with respect to the reference. Interesting, the obtained 2DEG isolation is stable up to 900 °C. Shiu et al. [32] found that ion implantation with oxygen ions produces a sheet resistance of 10^{12} Ω/sq stable up to 450 °C, but a dramatic decrese to about 100 Ω/sq occurs at temperature of 850 °C. In previous work, Roccaforte et al. [33] reported that, using nitrogen ion implantation, a sheet resistance of 10^{11} Ω/sq, stable at 750 °C was achieved. The sheet resistance is reduced of several orders of magnitude at 850 °C. Similar sheet resistance was found by Boudinov et al. [34] with a thermal stability up to 900 °C, obtained by MeV implantation of light ions of H, Li C and O. In this study we showed that also using Ar ion implantation at the fluence of 7×10^{13} cm^{-2} stable isolation of the 2DEG up to 900 °C can be obtained.

Conclusions

In this work we adopted a time and cost-saving methodology for the study of 2DEG isolation in $Al_{0.2}Ga_{0.8}N$/GaN heterostructure by Ar ion implantation. The methodology is based on the analysis, by photoluminescence spectroscopy, of the peak assigned to the radiative recombination of pairs at the BE and on the capacitance-voltage profiling of ion implanted and then post-annealed samples. The present study was conducted at the wafer level without the use of test structures that require the

fabrication of photolithographic metal pads for the ohmic contacts necessary for electrical characterization. We have shown that argon ion implantation at the energies of 15, 22.5 and 60 keV and fluence of 7×10^{13} cm^{-2} produces a significant reduction of the PL intensity of the BE peak. This finding is confirmed by a significant reduction of the 2DEG carrier density. The reduction of carrier density was found about six orders of magnitude with respect to the reference sample. The isolation was found stable at temperature up to 900°C. The methodology can be extended to the study of other ion implanted species. In a future work, the methodology described here will be extended to the study of the isolation effects on the 2DEG by carbon and iron ion implantation, comparing the results with those obtained by argon. The actual study has important technological implications, since shows that Ar ion implantation is able to produces stable isolation up to 900 °C. Implant conditions necessary for an effective electrical isolation of AlGaN/GaN 2DEG by ion implantation were also described.

Acknowledgements

The Project "Sviluppo di semiconduttori ad ampia banda proibita per dispositivi di potenza e telecomunicazione avanzata” CUP: E65F21002570005 – D.M. n. 1062 del 10 agosto 2021 Asse IV, Azione IV.4 “Dottorati e contratti di ricerca su tematiche dell'innovazione" del PON “R&I” 2014-2020 is acknowledged for financial support.

References

[1] N. Herbecq, I.R. Jeune, A. Linge, M. Zegaoui, P.O. Jeannin, N. Rouger, F. Medjdoub, Above 2000V breakdown voltage at 600 K GaN-on-silicon high electron mobility transistors, Phys. Status Solidi A 213 (2016), 873–877.

[2] T. Ueda, Y. Uemoto, T. Tanaka, D. Ueda, GaN transistors for power switching and millimeter-wave applications, Int. J. High Speed Electron. Syst. 19 (2009), 145–152.

[3] F. Ren, S.J. Pearton, Recent advances in wide-bandgap semiconductor biological and gas sensors, Semiconductor Device-Based Sensors for Gas, Chemical, and Bio Applications, CRC Press, Boca Raton London New York, (2011), 43–96.

[4] B. Li, X. Tang, J. Wang, K.J. Chen, Optoelectronic devices on AlGaN/GaN HEMT platform, Phys. Status Solidi A 213 (2016), 1213–1221.

[5] H. Sun, A.R. Alt, S. Tirelli, D. Marti, H. Benedickter, E. Piner, C.R. Bolognesi, Nanometric AlGaN/GaN HEMT performance with implant or mesa isolation, IEEE Electron Device Lett. 32 (2011), 1056–1058.

[6] U.K. Mishra, L. Shen, T.E. Kazior, Y.-F. Wu, GaN-based RF power devices and amplifiers, Proc. IEEE. 96 (2008), 287–305.

[7] F. Roccaforte, P. Fiorenza, R. Lo Nigro, F. Giannazzo, G. Greco, Physics and technology of gallium nitride materials for power electronics, Riv. Del Nuovo Cim. 41 (2018) 625-681 DOI: 10.1393/ncr/i2018-10154-x)

[8] F. Roccaforte, P. Fiorenza, G. Greco, R. Lo Nigro, F. Giannazzo, F. Iucolano, M. Saggio, Emerging trends in wide band gap semiconductors (SiC and GaN) technology for power devices, Microelectron. Eng.187-188, (2018) 66-77.

[9] X. Ding, Y. Zhou and J. Cheng, "A review of gallium nitride power device and its applications in motor drive," in CES Transactions on Electrical Machines and Systems 3 (2019), 54-64 doi: 10.30941/CESTEMS.2019.00008.

[10] A. M. Nahhas, Review of AlGaN/GaN HEMTs Based Devices. American Journal of Nanomaterials, 7 (2019), 10-21 http://pubs.sciepub.com/ajn/7/1/2

[11] F. Zeng, J.X. An, G. Zhou, W. Li, H. Wang, T. Duan, L. Jiang, H. Yu, A Comprehensive Review of Recent Progress on GaN High Electron Mobility Transistors: Devices, Fabrication and Reliability. Electronics 7 (2018), 377. https://doi.org/10.3390/electronics7120377

[12] M. Alathbah, K. Elgaid, Miniature Mesa Extension for a Planar Submicron AlGaN/GaN HEMT Gate Formation. Micromachines 13 (2022), 2007. https://doi.org/10.3390/mi13112007

[13] M. Sun, H.-S. Lee, B. Lu, D. Piedra, T. Palacios, Comparative breakdown study of mesa and ion-implantation-isolated AlGaN/GaN high-electron-mobility transistors on Si substrate, Appl. Phys. Express 5 (2012), 074202, 10.1143/APEX.5.074202

[14] Y. Li, G.I. Ng, S. Arulkumaran, Z.H. Liu, K. Ranjan, K.S. Ang, P.P. Murmu, and J. Kennedy, Improved planar device isolation in AlGaN/GaN HEMTs on Si by ultra-heavy $^{131}Xe^{+}$ implantation. Phys. Status Solidi A, 214 (2017), 1600794. https://doi.org/10.1002/pssa.201600794

[15] S. Arulkumaran, K. Ranjan, G. I. Ng, John Kennedy, P. P. Murmu, T. N. Bhat, S. Tripathy, Thermally stable device isolation by inert gas heavy ion implantation in AlGaN/GaN HEMTs on Si. Journal of Vacuum Science & Technology B 34 (4) (2016), 042203. https://doi.org/10.1116/1.4955152

[16] A. Taube, E. Kamińska, M. Kozubal, J. Kaczmarski, W. Wojtasiak, J. Jasiński, M.A. Borysiewicz, M. Ekielski, M. Juchniewicz, J. Grochowski, M. Myśliwiec, E. Dynowska, A. Barcz, P. Prystawko, M. Zając, R. Kucharski, A. Piotrowska, Ion implantation for isolation of

AlGaN/GaN HEMTs using C or Al. Phys. Status Solidi A 212 (2015), 1162-1169. https://doi.org/10.1002/pssa.201431724

[17] C. F. Lo, T. S. Kang, L. Liu, C. Y. Chang, S. J. Pearton, I. I. Kravchenko, O. Laboutin, J. W. Johnson, F. Ren; Isolation blocking voltage of nitrogen ion-implanted AlGaN/GaN high electron mobility transistor structure. Appl. Phys. Lett. 97 (26), (2010), 262116.

[18] J. -Y. Shiu et al., "Oxygen Ion Implantation Isolation Planar Process for AlGaN/GaN HEMTs," in IEEE Electron Device Letters, 28 (6), (2007), 476-478 doi: 10.1109/LED.2007.896904.

[19] K. Pągowska, M. Kozubal, A. Taube, R. Kruszka, M. Kaminski, N. Kwietniewski, M. Juchniewicz, A. Szerling, The interplay between damage and chemical induced isolation mechanism in Fe^{+} implanted AlGaN/GaN HEMT structures, *Mater Sci Semicond Process* 127 (2021), 105694. https://doi.org/10.1016/j.mssp.2021.105694

[20] H. Umeda, T. Takizawa, Y. Anda, T. Ueda and T. Tanaka, High-Voltage Isolation Technique Using Fe Ion Implantation for Monolithic Integration of AlGaN/GaN Transistors, in IEEE Transactions on Electron Devices, 60 (2), (2013), 771-775, doi: 10.1109/TED.2012.2230264.

[21] S. Tan, X. Deng, B. Zhang, et al. Thermal stability of F ion-implant isolated AlGaN/GaN heterostructures. Sci. China Phys. Mech. Astron. 61 (2018), 127311 https://doi.org/10.1007/s11433-018-9312-7

[22] Y.C. Lin, S.H. Chen, P.H. Lee, K.H. Lai, T.J. Huang, E.Y. Chang, H.-T Hsu, Gallium Nitride (GaN) High-Electron-Mobility Transistors with Thick Copper Metallization Featuring a Power Density of 8.2 W/mm for Ka-Band Applications. Micromachines 11 (2020), 222 https://doi.org/10.3390/mi11020222

[23] Y.-N. Zhong, S.-W. Tang, Y.-M. Hsin, Determination of Suitable Indicators of AlGaN/GaN HEMT Wafer Quality Based on Wafer Test and Device Characteristics. Phys. Status Solidi A, 215 (2018), 1700628 https://doi.org/10.1002/pssa.201700628

[24] J. Ziegler, The Stopping and Range of Ions in Matter, SRIM-2013.00 software http://www.srim.org.

[25] M. Takahashi, A. Tanaka, Y. Ando, H. Watanabe, M. Deki, M. Kushimoto, S. Nitta, Y. Honda, K. Shima, K. Kojima, S.F. Chichibu, K.J. Chen, and H. Amano, Suppression of Green Luminescence of Mg-Ion-Implanted GaN by Subsequent Implantation of Fluorine Ions at High Temperature, Phys. Status Solidi B 257 (2020), 1900554 DOI: 10.1002/pssb.201900554

[26] S.F. Chichibu, K. Shima1, K. Kojima, S. Takashima, K. Ueno, M. Edo, H. Iguchi, T. Narita, K. Kataoka, S. Ishibashi and A. Uedono, Room temperature photoluminescence lifetime for the near-band-edge emission of epitaxial and ion-implanted GaN on GaN structures, Jpn. J. Appl. Phys. 58 (2019) SC0802 DOI 10.7567/1347-4065/ab0d06

[27] M. Usman, A. Hallén, A. Nazir, Ion implantation induced nitrogen defects in GaN, J. Phys. D: Appl. Phys. 48 (2015), 455107 doi:10.1088/0022-3727/48/45/455107

[28] H. Sakurai, T. Narita, K. Kataoka, K. Hirukawa, K. Sumida, S. Yamada, K. Sierakowski, M. Horita, N. Ikarashi, M. Bockowski, Effects of the sequential implantation of Mg and N ions into GaN for p-type doping, Appl. Phys. Express 14 (2021), 111001 DOI 10.35848/1882-0786/ac2ae7

[29] F. Roccaforte, F. Giannazzo, G. Greco, Ion Implantation Doping in Silicon Carbide and Gallium Nitride Electronic Devices. Micro 2 (2022), 23-53 https://doi.org/10.3390/micro2010002

[30] F. Iucolano, F. Roccaforte, A. Alberti, C. Bongiorno, S. Di Franco, V. Raineri, Temperature dependence of the specific resistance in Ti⁄Al⁄Ni⁄Au contacts on n-type GaN. J. Appl. Phys., 12 (2006), 123706. https://doi.org/10.1063/1.2400825

[31] Y. Zhang, I. P. Smorchkova, C. R. Elsass, S. Keller, J- P. Ibbetson, S. Denbaars, Umesh K. Mishra, J. Singh, Charge control and mobility in AlGaN/GaN transistors: Experimental and theoretical studies. J. Appl. Phys. 87 (2000), 7981–7987. https://doi.org/10.1063/1.373483

[32] J.-Y. Shiu, J.-C. Huang, V. Desmaris, C.-T. Chang, C.-Y. Lu, K. Kumakura, T. Makimoto, H. Zirath, N. Rorsman, E.Y. Chang, Oxygen Ion Implantation Isolation Planar Process for AlGaN/GaN HEMTs. IEEE Electron Device Lett. 28 (2007), 476–478.

[33] F. Roccaforte, F. Iucolano, F. Giannazzo, G. Moschetti, C. Bongiorno, S. Di Franco, V. Puglisi, G. Abbondanza, V. Raineri, Influence of Thermal Annealing on Ohmic Contacts and Device Isolation in AlGaN/GaN Heterostructures. Mater. Sci. Forum, 615-617 (2009), 967–970.

[34] H. Boudinov, S.O. Kucheyev, J.S. Williams, C. Jagadish, G. Li, Electrical isolation of GaN by MeV ion irradiation. Appl. Phys. Lett. 78, (2001), 943–945.